Amino-Terminal Residues 1−45 of the *Escherichia coli* Pyruvate Dehydrogenase Complex E1 Subunit Interact with the E2 Subunit and Are Required for Activity of the Complex but Not for Reductive Acetylation of the E2 Subunit†

Yun-Hee Park, Wen Wei, Leon Zhou, Natalia Nemeria,* and Frank Jordan*

Department of Chemistry, Rutgers, the State University of New Jersey, Newark, New Jersey 07102

Received May 13, 2004; Revised Manuscript Received August 2, 2004

ABSTRACT: While N-terminal amino acids 1−55 are not seen in the structure of the *Escherichia coli* pyruvate dehydrogenase complex E1 subunit (PDHc-E1), mass spectrometric analysis indicated that this amino-terminal region of PDHc-E1 was protected by PDHc-E2. Hence, five deletion constructs of PDHc-E1 were created, Δ6−15, Δ16−25, Δ26−35, Δ36−45, and Δ46−55, along with single-site substitutions at Asp7, Asp9, Pro10, Ile11, Glu12, Thr13, Arg14, and Asp15. The decarboxylation of pyruvate and the ability of PDHc-E1 to dimerize are not affected by any of the deletions or substitutions. While Δ46−55 and the Pro10Ala, Ile11Ala, and Thr13Ala variants could form a complex with PDHc-E2, and produced NADH in the overall assay, Δ16−25, Δ26−35, and Δ36−45 and the Asp7Ala, Asp9Ala, Glu12Gln, Glu12Asp, Arg14Ala, and Asp15Ala variants failed in both respects. Remarkably, all constructs of PDHc-E1 from *E. coli*, as well as PDHc-E1 from *Mycobacterium tuberculosis*, could carry out reductive acetylation of the *E. coli* lipoyl domain, but only constructs of the *E. coli* PDHc-E1 could reductively acetylate *E. coli* PDHc-E2. It was concluded that there are at least two loci of interaction between the PDHc-E1 and PDHc-E2 subunits: (1) the thiamin diphosphate-bound substrate on PDHc-E1 and the lipoylamide of PDHc-E2, as reflected by the ability to reductively acetylate the latter; and (2) amino terminal residues 1−45 of PDHc-E1 with regions of PDHc-E2 (so far undefined for the *E. coli* complex), as reflected by the overall activity of the entire complex. These studies add important information regarding recognition within this multienzyme complex class with an α_2 E1 assembly.

The pyruvate dehydrogenase multienzyme complex (PDHc) isolated from *Escherichia coli* (*1*−*4*) consists of three subunits, thiamin diphosphate (ThDP)[1] dependent pyruvate dehydrogenase E1 [PDHc-E1 (*5*)], dihydrolipoamide acetyltransferase E2 with covalently bound lipoamide [PDHc-E2 (*6*); in this study, a construct with a single lipoyl domain was used, but this construct had earlier been shown to have properties virtually identical to those of the enzyme with three lipoyl domains (*7*, *8*)], and dihydrolipoamide dehydrogenase PDHc-E3 with FAD and NAD^+ (*9*), and carries out the reactions shown in eqs 1−5.

$$\text{pyruvate} + \text{E1}-\text{ThDP}-\text{Mg}^{2+} \rightarrow \text{E1}-\text{hydroxyethylidene}-\text{ThDP}-\text{Mg}^{2+} + \text{CO}_2 \quad (1)$$

$$\text{E1}-\text{hydroxyethylidene}-\text{ThDP}-\text{Mg}^{2+} + \text{E2}-\text{lipoamide} \rightarrow \text{E1}-\text{ThDP}-\text{Mg}^{2+} + \text{E2}-\text{acetyldihydrolipoamide} \quad (2)$$

$$\text{E2}-\text{acetyldihydrolipoamide} + \text{CoA} \rightarrow \text{E2}-\text{dihydrolipoamide} + \text{acetyl-CoA} \quad (3)$$

$$\text{E2}-\text{dihydrolipoamide} + \text{E3}-\text{FAD} \rightarrow \text{E2}-\text{lipoamide} + \text{E3}-\text{FADH}_2 \quad (4)$$

$$\text{E3}-\text{FADH}_2 + \text{NAD}^+ \rightarrow \text{E3}-\text{FAD} + \text{NADH} \quad (5)$$

We sought to identify the loci of interaction between PDHc-E1 and PDHc-E2, and as a first study directed at the PDHc-E1 partner, we have carried out deletion analysis of its N-terminal region. The motivation for selecting this region is multifold. The recently reported high-resolution crystal structure indicated that there were three regions spanning residues 1−55, 401−413, and 541−557 which did not lead to interpretable electron density, presumably due to the mobility of these regions (*10*). Nevertheless, H407, located in the second missing region, was found to be critical for catalysis, probably in the reductive acetylation of lipoamide of the PDHc-E2 subunit (*11*), suggesting that the other two mobile regions, especially N-terminal residues 1−55, comprising the largest fragment not seen in the structure, may also be important. We here show using mass spectroscopic measurements that the amino-terminal region of PDHc-E1 is protected from trypsinolysis by the PDHc-E2 subunit. Earlier, de Kok and co-workers reported for PDHc-E1 from *Azotobacter vineladii* (an enzyme with a sequence significantly identical and similar to that of *E. coli* PDHc-E1) that

† Supported by NIH Grant GM-62330.

* To whom correspondence should be addressed. Telephone: (973) 353-5470. Fax: (973) 353-1264. E-mail: nemeria@newark.rutgers.edu and frjordan@newark.rutgers.edu.

[1] Abbreviations: ThDP, thiamin diphosphate; PDHc-ec, pyruvate dehydrogenase complex from *E. coli*; PDHc-E1ec, first ThDP-dependent subunit of PDHc; PDHc-E2, second subunit of the complex, in this paper carrying a single lipoyl domain; PDHc-E1−PDHc-E2, complex formed between the two subunits; PDHc-E1mt, first ThDP-dependent subunit of PDHc from *Mycobacterium tuberculosis*; DCPIP, 2,6-dichlorophenolindophenol; FT-ICR MS, Fourier transform ion cyclotron resonance mass spectrometry; MALDI-TOF MS, matrix-assisted laser desorption ionization time-of-flight mass spectrometry; DSC, differential scanning calorimetry.

10.1021/bi049027b CCC: $27.50
Published on Web 10/12/2004

the 50 N-terminal residues are required in the binding of PDHc-E1 to PDHc-E2 (*12*−*14*).

Hence, five deletion constructs of PDHc-E1 were created, Δ6−15, Δ16−25, Δ26−35, Δ36−45, and Δ46−55. While the decarboxylation of pyruvate and the ability of PDHc-E1 to dimerize are not affected by any of the deletions, the ability of the Δ16−25, Δ26−35, and Δ36−45 constructs, but not of the Δ46−55, to form a complex with PDHc-E2, as well as to produce NADH when used to reconstitute the complex, is severely compromised. Because of the difficulty in the expression of the Δ6−15 construct, single-site substitutions were introduced into this region, thereby narrowing the locus of interaction to residues 7−45 of PDHc-E1.

EXPERIMENTAL PROCEDURES

Materials. Plasmid pGS878 encoding the PDHc-E1 subunit and the JRG 3456 cells (PDHc-E1 deficient) were kindly provided by J. Guest of the University of Sheffield (Sheffield, United Kingdom). The Wizard 373 DNA purification system was from Promega Inc. (Madison, WI). The QuikChange site-directed mutagenesis kit was from Stratagene (La Jolla, CA). T4 DNA ligase was from New England BioLabs (Beverly, MA). The QIAquick Gel Extraction Kit was from Qiagene Inc. (Valencia, CA). The primers for mutagenesis were from Integrated DNA Technologies, Inc. (Coralville, IA). Sequencing-grade modified trypsin was from Promega.

Construction of the Δ6−15, Δ16−25, Δ26−35, Δ36−45, and Δ46−55 Deletion Variants of PDHc-E1. Plasmid DNA was purified according to the protocol outlined for the Wizard 373 DNA purification system. Mutagenesis reactions were carried out using the QuikChange site-directed mutagenesis kit. The polymerase chain reaction was carried out for 17 cycles in a Mini-cycler (MJ Research, Inc.) using double-stranded pGS878 DNA and two synthetic mutagenic primers annealed to different strands of the DNA. The strategy for the design of mutagenic primers was that from the instruction manual to ExSite PCR-Based site-directed mutagenesis (Stratagene). Both mutagenic primers were 5′-phosphorylated. The following synthetic 2′-deoxyoligonucleotides were used as mutagenic primers: 5′-TGGCTCCAGGCGATCGAATCGGTC-3′ and 5′-CGGGAAACGTTCAGACATGATCCT-3′ for Δ6−15, 5′-GAAGAAGGTGTTGAGCGTGCTCAG-3′ and 5′-GTCGCGAGTTTCGATCGGATCCAC-3′ for Δ16−25, 5′-ATCGACCAACTGCTTGCTGAAGCC-3′ and 5′-ACGGATGACCGATTCGATCGCCTG-3′ for Δ26−35, 5′-GGCGGTGTAAACGTAGCCGCAGGC-3′ and 5′-CAGATACTGAGCACGCTCAACACCTTC-3′ for Δ36−45, 5′-ATCAGCAACTACATCAACACCATCCCC-3′ and 5′-TTTGCGGGCTTCAGCAAGCAGTTGGTC-3′ for Δ46−55.

The 8.3 kb DNA fragment PCR product encoding PDHc-E1 was purified on a 0.8% preparative agarose gel using the QIAquick Gel Extraction Kit. The purified DNA was ligated by T4 DNA ligase under the conditions specified by the manufacturer. For confirmation of the desired sequences, XL1-Blue supercompetent cells were transformed with recirculized DNA and ampicillin-resistant colonies were selected. The presence of deletions was verified by sequencing of the PDHc-E1 gene with the primers reported previously (*15*).

Construction of Singly Substituted Amino-Terminal Variants of PDHc-E1. Mutagenesis reactions were carried out using double-stranded pGS878 DNA with two synthetic mutagenic primers complementary to opposite strands of DNA, and the reagents supplied with the QuikChange site-directed mutagenesis kit for 16 cycles. The following synthetic 2′-deoxyoligonucleotides and their complements were used as mutagenic primers (mutant codons in boldface type): 5′-GAACGTTTCCCAAAT**GCC**GTGGATCCGATC-3′ (Asp7Ala), 5′-CCAAATGACGTG**GCT**CCGATCGAAACTCG-3′ (Asp9Ala), 5′-CCAAATGACGTGGAT**GCG**ATCGAAACTCGC-3′ (Pro10Ala), 5′-GACGTGGATCCG**GC-C**GAAACTCGCGAC-3′ (Ile11Ala), 5′-CGTGGATCCGATC**GCA**ACTCGCGACTG-3′ (Glu12Ala), 5′-GACGTGGATCCGATC**GAC**ACTCGCGACTGG-3′ (Glu12Asp), 5′-GACGTGGATCCGATC**CAA**ACTCGCGACTGG-3′ (Glu12Gln), 5′-GATCCGATCGAA**GCT**CGCGACTGGCTC-3′ (Thr13Ala), 5′-GTGGATCCGATCGAAACT**GCC**GACTGGCTC-3′ (Arg14Ala), and 5′-CGATCGAAACTCGC**GC-C**TGGCTCCAGG-3′ (Asp15Ala).

Expression and Purification of Parental PDHc-E1 and Its Variants. Expression of parental PDHc-E1, its N-terminal deletion, and singly substituted variants followed the procedure described previously (*15*). Purification of parental PDHc-E1 and its N-terminal deletion variants was carried out using an HPLC system described previously (*16*). Purification of singly substituted variants was carried out with an ÅKTA FPLC system (Amersham Pharmacia Biotech) and an XK26 HiLoad 26/10 Q Sepharose High Performance column. PDHc-E1 and its variants were eluted with a linear gradient of NaCl (from 0.20 to 1.0 M) in 20 mM KH_2PO_4 buffer (pH 7.5).

Expression and purification of the independently expressed lipoyl domain and of single-lipoyl domain E2 (PDHc-E2) were described elsewhere (*17*).

Activity and Related Measurements. The activity of parental PDHc-E1 and its variants was measured by using them in reconstitution of the entire complex with saturating concentrations of the PDHc-E2−PDHc-E3 subcomplex (the mass ratio of PDHc-E1 to the subcomplex was 1:5) using a Cary 300 Bio UV−visible spectrophotometer (Varian), monitoring the pyruvate-dependent reduction of NAD^+ at 340 nm (*15*). The activity of parental PDHc-E1 and its variants was also measured after reconstitution of the complex from PDHc-E1, PDHc-E2, and PDHc-E3 subunits expressed independently using a PDHc-E1:PDHc-E2:PDHc-E3 mass ratio of 1:1:0.5, and the incubation medium reported previously (*17*).

The E1-specific activity of the parental and variant PDHc-E1s was measured in the model reaction with 2,6-dichlorophenolindophenol (2,6-DCPIP) as the external oxidizing agent by monitoring the reduction of 2,6-DCPIP at 600 nm (*15*).

Size-Exclusion Chromatographic Determination of the M_r of PDHc-E1 and Its Variants. A TSK G3000-SW size-exclusion column equilibrated with 50 mM KH_2PO_4 buffer (pH 7.0) containing 0.15 M NaCl was used for the measurements. The column was calibrated with the following standards (M_r values listed): thyroglobulin (669 000), ferritin (440 000), catalase (232 000), aldolase (158 000), bovine serum albumin (67 000), ovalbumin (43 000), chymotrypsinogen (25 000), and ribonuclease A (13 700). PDHc-E1 or its deletion variants (1 mg/0.2 mL) were dissolved in the

equilibrating buffer and applied to the column at a flow rate of 1 mL/min.

Differential Scanning Calorimetry. DSC measurements were carried out using a 2920 differential scanning calorimeter (TA Instrument, Inc., New Castle, DE) at a scan rate of 1 °C/min in 20 mM KH_2PO_4 buffer (pH 7.0). Samples (10 mg/mL) were scanned from 15 to 100 °C, and the midpoint melting temperature (T_m) was determined.

Multiangle Laser Light Scattering Experiments. Multiangle laser light scattering experiments were carried out using a Dawn EOS instrument (Wyatt Technology, Santa Barbara, CA). The refractive index increment (d*n*/d*c*) value was determined with an Optilab DSP Interferometric refractometer (Wyatt Technology). Aliquots of the PDHc-E1−PDHc-E2 complex that eluted from an analytical size-exclusion column in 50 mM KH_2PO_4 buffer (pH 7.0) containing 0.15 M NaCl were injected into the instrument in a volume of 2 mL. The enzyme concentration was 10−90 μg/mL for the refractometer and 1−9 μg/mL for the light scattering experiments. All experiments were carried out at room temperature. The M_r value was calculated by using the Astra software for Windows supplied by the manufacturer.

Reductive Acetylation of the Lipoyl Domain and of PDHc-E2 Monitored by MALDI-TOF Mass Spectrometry. To monitor reductive acetylation of the independently expressed lipoyl domain, PDHc-E1 or its deletion variants (0.1 μM) were incubated in 20 mM HEPES buffer (pH 7.0) with 2 mM $MgCl_2$, 0.20 mM ThDP, 2.0 mM pyruvate, and 0.30 or 0.60 mM lipoyl domain in a total volume of 0.10 mL at 25 °C. After 30 s and 1, 2, 15, 30, and 40 min, 1 μL aliquots were withdrawn and mixed with 1 μL of sinapinic acid on the target plate. To monitor reductive acetylation of PDHc-E2, PDHc-E1 or its deletion variants (0.1 μM) were incubated with PDHc-E2 (2 mg/mL) in 0.1 mL of 20 mM Tris buffer (pH 8.5), containing 0.30 M NaCl. After 30 min at 25 °C, trypsin was added to digest PDHc-E2 [200:1 PDHc-E2:trypsin ratio (w/w)]. The reaction was stopped after incubation for 40 min by the addition of benzamidine hydrochloride (0.15 mg/mL), and samples were diluted 10-fold with 0.1% trifluoroacetic acid. Aliquots (1 μL) were withdrawn and mixed with 1 μL of sinapinic acid on the target plate. Mass spectra were acquired on a Voyager-DE PRO MALDI-TOF (PerSeptive Biosystems, Framingham, MA) mass spectrometer equipped with a nitrogen laser to desorb and ionize samples. An accelerating voltage of 25 kV was used, and the spectrometer was calibrated using ubiquitin (molecular mass of 8566 Da) for determination of the mass of the lipoyl domain.

Tryptic Digestion of PDHc-E1 for FT-ICR MS Analysis. For the tryptic digestion, 150 μL of PDHc-E1 (5 mg/mL) was mixed with 7.5 μL of trypsin (0.10 mg/mL) in 50 mM Tris buffer (pH 8.2) [PDHc-E1:trypsin ratio of 1000:1 (w/w)]. After incubation for 3 h at 25 °C, 0.10 mL of benzamidine hydrochloride (0.15 mg/mL) was added to terminate the proteolysis. Prior to the mass spectrometric analysis, the nonvolatile buffer was exchanged for buffer A, which is compatible with mass spectrometry. To the above incubate was added 1 mL of buffer A, consisting of a 50/50/0.20 (v/v) mixture of methanol, 20 mM ammonium bicarbonate (pH 8.9), and 0.2% formic acid, followed by concentration with a Centricon YM-3 unit (Millipore), and then the entire sequence was repeated once. The resulting sample was diluted to 150 μL with buffer A. To study the time course of proteolysis, PDHc-E1 was incubated with trypsin under the conditions presented above; then aliquots were withdrawn after 10 and 30 min and 1, 2, and 3 h, and the proteolysis was terminated by addition of benzamidine hydrochloride. The buffer exchange was as presented above.

Tryptic Digestion of the Mixture of PDHc-E1 and PDHc-E2. For the tryptic digestion, 30 μL of PDHc-E1 (17.9 mg/mL) was mixed with 70 μL of PDHc-E2 [4.8 mg/mL in 50 mM Tris buffer (pH 8.2) containing 0.30 M NaCl]. To this mixture were added $MgCl_2$ (2 mM), ThDP (0.20 mM), and pyruvate (2 mM). After incubation for 30 min at 25 °C, an aliquot of 10 μL of trypsin (0.10 mg/mL) was added. The tryptic digestion was stopped after incubation for 2 h by addition of 0.1 mL of benzamidine hydrochloride (0.15 mg/mL). The buffer was exchanged as described above. As controls, the tryptic digestions of PDHc-E1 and PDHc-E2 were carried out in parallel. The peptide profiles obtained separately for PDHc-E1 and PDHc-E2 were used as baseline controls.

FT-ICR MS Analysis of the Digested Proteins. Mass spectrometric analysis was carried out on a Bruker 4.7 T Fourier transform ion cyclotron resonance mass spectrometer (FT-ICR MS). The samples were introduced into the mass spectrometer through a Cole-Parmer syringe pump at a flow rate of 100 μL/h. Mass spectra were acquired with electrospray in the positive ionization mode. To achieve high accuracy in the mass measurement, the mass spectrometer was calibrated using Agilent ES Tuning Mix over a mass-to-charge ratio of 300−2500. The acquired mass spectra were deconvoluted, and the mass-to-charge ratio of the monoisotopic peaks of various tryptic peptides was recorded. Identification of these peptides was accomplished by matching their monoisotopic signals from the deconvoluted mass spectra to the theoretical monoisotopic values of the expected peptides using the Sequence Editor of Bruker's biotool program, version 2.0.

RESULTS

Mass Spectral Mapping of the Binding Interface on PDHc-E1 in the PDHc-E1−PDHc-E2 Complex. Peptide maps were generated for the PDHc-E1 and PDHc-E2 subunits separately and for their mixture with peptide identification provided by FT-ICR MS after tryptic digestion. More than 50 peptide fragments which originated from PDHc-E1 were detected by FT-ICR MS (49 are presented in Table 1), and their masses match perfectly the masses of the predicted peptide fragments generated on the basis of the amino acid sequence of the PDHc-E1 subunit (886 amino acids, starting with serine). The grand average error is 12.2 ppm, indicating the high standard of mass measurement accuracy. Very importantly, peptides encompassing amino acid residues 1−55, 401−413, and 541−557, for which no electron density was found in the crystal structure of PDHc-E1 with ThDP bound (*10*), were identified by mass spectrometry (Table 1). For the region of interest in this paper, N-terminal residues 1−55, the following peptide fragments were found: 1−14, 15−31, 15−44, 32−44, 45−79, 45−80, 46−79, and 46−80 (suggesting that this region of PDHc-E1 is probably exposed and is located on the protein surface).

Table 1: FT-ICR MS Analysis of the Tryptic Digest of PDHc-E1[a]

residue numbers	theoretical monoisotope mass (Da)	experimental monoisotope mass (Da)	error (Da)	error (ppm)
631−676	5093.392	5093.47656	0.085	16.6
767−805	4461.065	4461.10771	0.043	9.6
677−711	4167.902	4167.94927	0.047	11.3
677−710	4039.807	4039.82575	0.019	4.6
466−500	3978.063	3977.99005	−0.073	18.3
422−455	3972.928	3972.9728	0.045	11.3
45−80	3883.97	3884.02868	0.059	15.1
335−367	3797.823	3797.88412	0.061	16.1
46−80	3755.875	3755.92179	0.047	12.5
45−79	3727.869	3727.92081	0.052	13.9
424−455	3701.8	3701.84852	0.049	13.1
46−79	3599.774	3599.78615	0.012	3.4
436−465	3566.806	3566.83263	0.027	7.5
274−303	3529.818	3529.77044	−0.048	13.5
15−44	3512.826	3512.8739	0.048	13.6
127−156	3321.623	3321.64742	0.024	7.4
737−766	3282.652	3282.69888	0.047	14.3
157−181	2893.411	2893.44724	0.036	12.5
383−410	2892.528	2892.4701	−0.058	20.0
740−766	2890.424	2890.45361	0.030	10.2
222−247	2798.343	2798.39801	0.055	19.7
215−239	2744.285	2744.31663	0.032	11.5
835−858	2666.382	2666.41883	0.037	13.8
127−150	2648.273	2648.29743	0.024	9.2
129−150	2421.135	2421.16096	0.026	10.7
839−858	2154.111	2154.13429	0.023	10.8
515−533	2134.124	2134.1532	0.029	13.7
383−403	2102.083	2102.10745	0.024	11.6
748−766	2064.964	2064.97861	0.015	7.1
866−884	2055.111	2055.13499	0.024	11.7
15−31	2028.028	2028.0458	0.018	8.8
534−550	1963.939	1963.96297	0.024	12.2
458−472	1785.916	1785.95317	0.037	20.8
724−739	1719.027	1718.98058	−0.046	27.0
510−524	1694.968	1694.98401	0.016	9.4
1-−14	1673.801	1673.81794	0.017	10.1
712−725	1521.84	1521.85344	0.013	8.8
32−44	1502.809	1502.83261	0.024	15.7
711−723	1464.819	1464.83063	0.012	7.9
712−723	1336.724	1336.74112	0.017	12.8
874−884	1287.657	1287.67063	0.014	10.6
737−747	1235.699	1235.7093	0.010	8.3
515−524	1095.629	1095.63932	0.010	9.4
383−392	1065.655	1065.66628	0.011	10.6
393−403	1054.439	1054.45363	0.015	13.9
806−812	861.471	861.48128	0.010	11.9
740−747	843.47	843.48107	0.011	13.1
404−410	808.456	808.46405	0.008	10.0
240−247	801.471	801.48008	0.009	11.3
			average error	12.2

[a] In column 1 is listed the sequence assignment of the peptide. For example, 631−676 corresponds to the sequence of amino acids 631−676 inclusive in the PDHc-E1 subunit. Column 2 lists the theoretical mass predicted for this peptide, and column 3 lists the experimentally determined values of the monoisotopic peaks of the peptides. The difference between these two values, in either daltons or parts per million, is given in columns 4 and 5.

Limited tryptic hydrolysis of the PDHc-E2 subunit identified 27 peptide fragments. All of the experimentally determined peptide masses were in excellent agreement with the predicted values based on the amino acid sequence of PDHc-E2. The grand average error between the experimental and the predicted masses is 5.2 ppm (data not presented).

Next, a mixture of PDHc-E1 and PDHc-E2 was subjected to limited proteolysis by trypsin. The peptide map of the PDHc-E1 subunit trypsinized in the presence of PDHc-E2 is shown in Figure 1. Peptide fragments 1−14, 15−31, 32−44, 45−80, 46−79, and 46−80 were missing. The signal for the 15−44 peptide fragment was very weak compared to the signal observed with PDHc-E1 alone, clearly indicating that N-terminal amino acid residues 1−55 are important for the interaction with the PDHc-E2 subunit. Addition of ThDP (0.20 mM), $MgCl_2$ (2 mM), and pyruvate (2.0 mM) to a mixture of PDHc-E1 and PDHc-E2 enables reductive acetylation of the latter as also detected by MALDI-TOF MS (*11*, *17*). As seen in Figure 1, addition of ThDP, $MgCl_2$, and pyruvate does not affect the peptide map, indicating that residues 1−55 of PDHc-E1 are involved in the binding of PDHc-E1 to PDHc-E2. The region of PDHc-E1 protected by the presence of PDHc-E2 is clearly identified, demonstrating the power and potential of the FT-ICR MS method.

Characterization of the Amino-Terminal Deletion and Singly Substituted PDHc-E1 Variants. The plasmids encoding the Δ6−15, Δ16−25, Δ26−35, Δ36−45, and Δ46−55 deletion variants of PDHc-E1 were constructed as described in Experimental Procedures, and the proteins were expressed in JRG3456 (PDHc-E1 deficient) cells. According to SDS−PAGE, the Δ6−15 PDHc-E1 variant was weakly expressed, and attempts to purify the protein failed. This result and the unsuccessful attempts to express the PDHc-E1 with the six-His tag at the N-terminus (data not shown) suggest that the N-terminal region of the PDHc-E1 is sensitive to any perturbation. All other deletion variants were expressed at levels comparable to that obtained with the parental enzyme. The Δ46−55 variant behaves like parental PDHc-E1 when applied to a DEAE column (the retention time was ∼105−110 min, similar to that of parental PDHc-E1). The Δ16−25, Δ26−35, and Δ36−45 PDHc-E1 variants were eluted ∼20 min earlier than parental PDHc-E1 (retention time of ∼80 min). As seen in Figure 2, the amino acid sequence of the N-terminal region of PDHc-E1 from *E. coli* is highly negatively charged. In addition, the absence of this region in the X-ray structure of PDHc-E1 suggested that the region is highly flexible. Limited deletions of the N-terminal region resulted in a shorter retention time of the protein on the DEAE anion exchange column, implying that the negatively charged residues on the N-terminus are involved in ionic interactions with the column.

The activities of parental PDHc-E1 and its deletion variants measured with different assays are presented in Table 2. After reconstitution of the complex, compared with parental PDHc-E1, the Δ46−55 PDHc-E1 variant retained 83% activity according to the overall PDHc reaction assay and 100% activity according to the E1-specific DCPIP assay. The specific activities of the remaining three variants in the overall PDHc assay were drastically reduced: 1.3% (Δ16−25), 0.35% (Δ26−35), or none (Δ36−45) (Table 2). In the E1-specific DCPIP assay, the differences were modest; these three variants retain 20−50% of the PDHc-E1 activity.

Since we were unable to purify the Δ6−15 variant, plasmids encoding PDHc-E1 were created with single-site substitutions in this region: Asp7Ala, Asp9Ala, Pro10Ala, Ile11Ala, Glu12Ala, Glu12Asp, Glu12Gln, Thr13Ala, Arg14Ala, and Asp15Ala. All of the variants, except Glu12Ala, were expressed in JRG3456 cells and were purified in a manner similar to that for parental PDHc-E1. As shown in Table 2, of all the singly substituted variants, Pro10Ala and Ile11Ala display overall activity comparable

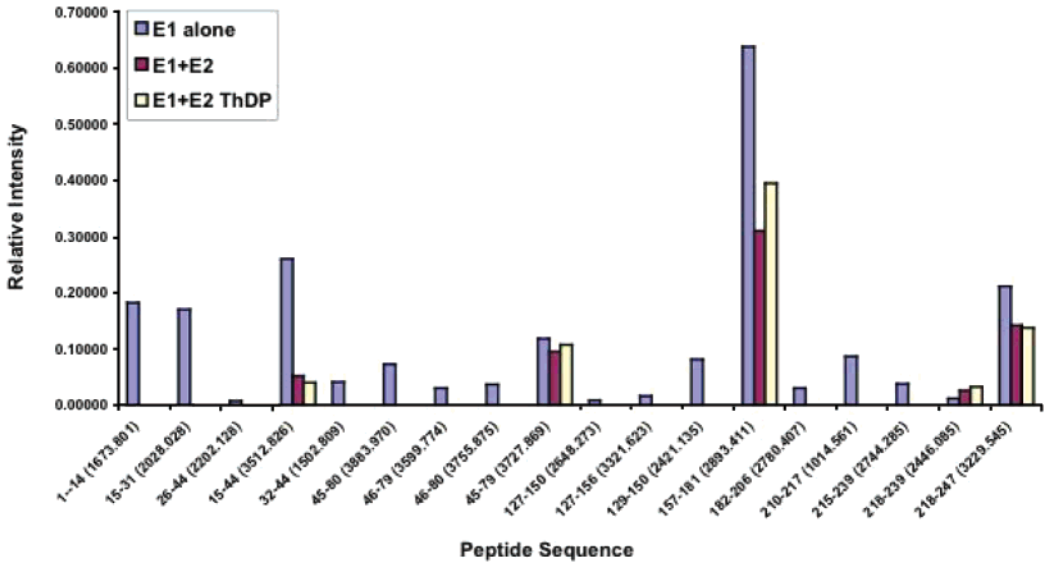

FIGURE 1: Tryptic peptides of *E. coli* PDHc-E1. In blue are shown the fragments resulting from digestion of PDHc-E1 alone and in maroon the PDHc-E1 peptides evident from a tryptic digest of the PDHc-E1−PDHc-E2 complex, and in yellow is shown the same experiment as in maroon but with ThDP, Mg(II), and pyruvate present. Zero intensities for peptides are below 0.0005.

E.coli	SERFPN**D**V**D**	**PIETRD**WLQA	IESVIREEGV	ERAQYLIDQL	LAEARKGGVN
A.vinelandii	MQDMQ**D**L**D**	**PIET**QEWLDS	LESLLDHEGE	ERAHYLLTRM	GELATRTGTQ
H.influenzae	MSEILKN**D**V**D**	**PIET**Q**D**WLQS	LDSLIREEGV	ERAQYIVEQV	IGQARTSGVS
M.leprae	GVASYLP**D**I**D**	**PEET**AEWLES	FDELLKHSGP	SRARYLILRL	LERAGEQRVT
M.tuberculosis	MASYLP**D**I**D**	**PEET**SEWLES	FDTLLQRCGP	SRARYLMLRL	LERAGEQRVA
N.meningitidis	MSTQLH**D**V**D**	**PIET**QEWLDA	LSSVLEYEGG	ERAQYLLENL	VKYCRDKGVR
P.aeruginosa	MQ**D**L**D**	**P**V**ET**QEWLDA	LESVLDREGE	DRAHYLMTRM	GELASRSGTQ
P.multocida	MSDMLKN**D**V**D**	**P**V**ET**N**D**WLLA	IDAVIREEGV	ERAQYIIEQL	MQHARANNVS
S.typhimurium	MSERFQN**D**V**D**	**PIET**R**D**WLQA	IESVIREEGV	ERAQYLIDQL	LSEARKGGVK
V.cholerae	MSDMKH**D**V**D**	AL**ET**QEWLAA	LESVVREEGV	ERAQYLLEQV	LEKARLDGVD
Y.pestis	MSERLNN**D**V**D**	**PIET**R**D**WLQA	IESVIREEGV	ERAQYLIDQV	LGEARKGGVS
B.aphidicola	MSENLYN**D**V**D**	**PIET**R**D**WVQA	IESVIRREGH	KRAHFLIEQV	LKTAKINRKE

FIGURE 2: Alignment of the N-terminal amino acid sequences of the bacterial pyruvate dehydrogenase complex E1 subunits using the BLAST program. Single substitutions reported in this paper on the *E. coli* enzyme as well as conserved residues are in boldface. The numbering adopts Ser as the first amino acid at the N-terminus: *E. coli*, *Escherichia coli*; *A. vinelandii*, *Azotobacter vinelandii*; *H. influenzae*, *Haemophilus influenzae*; *M. leprae*, *Mycobacterium leprae*; *M. tuberculosis*, *Mycobacterium tuberculosis*; *N. meningitidis*, *Neisseria meningitidis*; *P. aeruginosa*, *Pseudomonas aeruginosa*; *P. multocida*, *Pasteurella multocida*; *S. typhimurium*, *Salmonella typhimurium*; *V. cholerae*, *Vibrio cholerae*; *Y. pestis*, *Yersinia pestis*; and *B. aphidicola*, *Buchnera aphidicola.*

to that of parental PDHc-E1, 107 and 94%, respectively. Thr13Ala displayed 13%, Glu12Gln 3.3%, and Glu12Asp 2.3% of the activity of parental PDHc-E1. All other variants displayed drastically diminished activity (0.14−0.25%) or none (Asp9Ala) upon reconstitution of the complex. The effect of substitutions on E1-specific DCPIP activity was not significant [41−104%, with the exception of 10% activity for the Glu12Asp variant, much lower than with the other variants (Table 2)].

Effect of N-Terminal Deletions or Substitutions on the Ability of PDHc-E1 To Dimerize. The apparent relative molecular weight (M_r) of PDHc-E1 and its deletion variants was determined using a TSK G3000-SW size-exclusion column and conditions presented in Experimental Procedures (Figure 3A). PDHc-E1 is eluted from the column with a retention time of 15.8 min, which corresponds to a dimer with an M_r of 198 000 [mass of the PDHc-E1 subunit, 99 474 Da (*5*)]. An additional peak was observed with a retention time of 13.0 min and was identified as an aggregate of the PDHc-E1 subunit according to activity measurements. The small shoulder with a retention time of 17.4 min is believed to correspond to a PDHc-E1 monomer (M_r = 104 000). All three peaks were shown to consist of PDHc-E1 according to SDS−PAGE. From the size-exclusion chromatographic experiments, it was evident that the Δ16−25, Δ26−35, Δ36−45, and Δ46−55 variants were eluted as dimers (see Figure 3B for the result with the Δ16−25 variant), indicating that deletions in the N-terminal region of residues 16−55 do not abolish the assembly of the PDHc-E1 subunits into a dimer.

Similar size-exclusion HPLC experiments demonstrated that all of the singly substituted variants could dimerize as well.

Table 2: Specific Activities of PDHc-E1 with Deletions and Single-Amino Acid Substitutions in the Amino-Terminal Region

enzyme variant	pyruvate:NAD^+ oxidoreductase assay (% of parental)[a]	PDHc-E1-specific 2,6-DCPIP assay (% of parental)[b]
PDHc-E1	100	100
Δ16−25	1.3	37
Δ26−35	0.35	20
Δ36−45	0	50
Δ46−55	83	100
Asp7Ala	0.14	90
Asp9Ala	0	88
Pro10Ala	107	80
Ile11Ala	94	62
Glu12Asp	2.3	10
Glu12Gln	3.3	41
Thr13Ala	13	74
Arg14Ala	0.25	104
Asp15Ala	0.19	84

[a] The overall activity of the PDHc-E1 variants with the indicated deletions was measured by reconstitution with PDHc-E2−PDHc-E3 subcomplex [the activity of parental PDHc-E1 was 28.35 ± 1.53 μmol min^{-1} (mg of E1)$^{-1}$]. The activity of singly substituted variants was measured after reconstitution with independently expressed PDHc-E2 and PDHc-E3 subunits [the activity of parental PDHc-E1 was 34.9 ± 2.76 μmol min^{-1} (mg of E1)$^{-1}$]. [b] The E1-specific activity of parental PDHc-E1 was 0.385 ± 0.110 μmol min^{-1} (mg of E1)$^{-1}$.

A peak of variable size with a retention time of ~25 min was present in chromatograms of deletion variants of PDHc-E1 (panels B and D of Figure 3 present data for Δ16−25). This retention time corresponds to an M_r of less than 13 700, and probably represents a partially folded form of the PDHc-E1 monomer. That the peak does not represent a proteolytic fragment of PDHc-E1 was ruled out by experiments in which a cocktail of protease inhibitors was used throughout the experiments, and led to similar results. It was shown that ThDP reduced the size of the peak at 25 min by a factor of 3−4 (data not presented), while increasing the size of the 15.8 min peak corresponding to the Δ16−25 PDHc-E1 dimer. This suggests that ThDP shifts an equilibrium between species represented by the 25 and 15.8 min peaks, and also affirms that the peak with a retention time of 25 min most likely corresponds to a monomer of Δ16−25 PDHc-E1. ThDP appears in the chromatogram with a retention time of 27 min.

Physicochemical Evidence for Interaction of PDHc-E1 and PDHc-E2 and Effect of N-Terminal PDHc-E1 Deletions on this Interaction. The binding of PDHc-E1 and its deletion variants to PDHc-E2 was monitored using the TSK G3000-SW size-exclusion column followed by SDS−PAGE analysis of the components of the eluted peaks. PDHc-E1 (0.50 mg) was incubated with PDHc-E2 (0.50 mg; the molar subunit concentration was twice that of PDHc-E1) in a total volume of 0.20 mL at room temperature. After 40 min, the sample was centrifuged and the supernatant was applied to the HPLC column. The only visible peak corresponds to the PDHc-E1−PDHc-E2 complex (according to SDS−PAGE) and has a retention time of 11.8 min, extrapolating to an M_r of more than 600 000 (Figure 3C). This estimate of the M_r represents a lower limit since the analytical column that was used did not allow us to determine a reliable molecular weight for this high-M_r range. *It is to be noted that no peak corresponding to the PDHc-E2 subunit or any oligomers thereof could be observed when PDHc-E2 alone was subjected to the size-exclusion HPLC, presumably due its aggregation.*

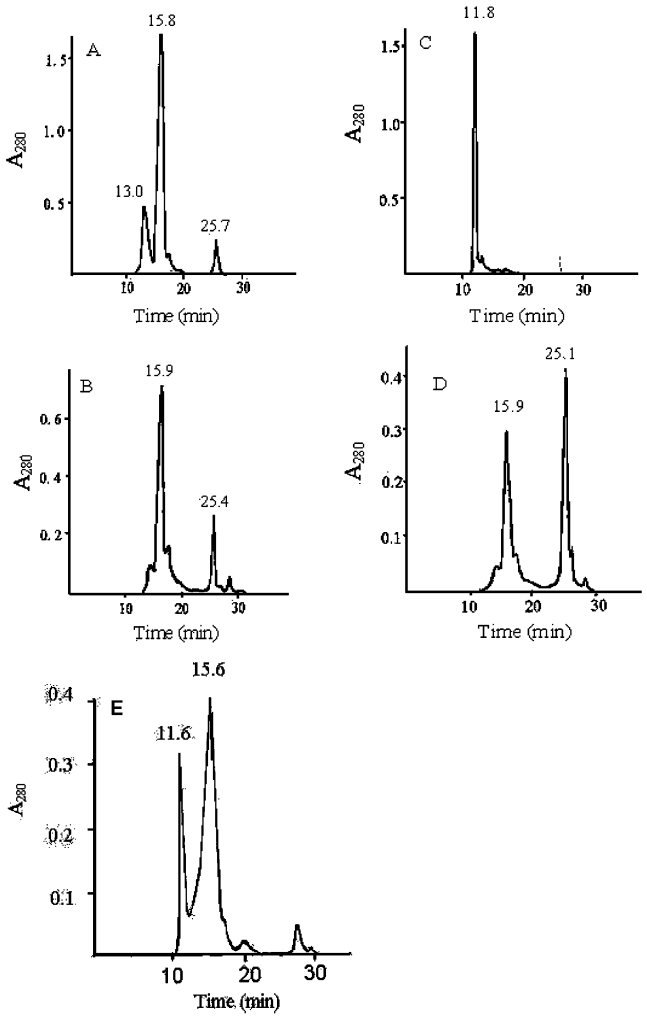

FIGURE 3: Size-exclusion HPLC evidence for dimerization of parental PDHc-E1 and its variants and for complexation with PDHc-E2: (A) parental PDHc-E1, (B) Δ16−25 PDHc-E1, (C) complex of parental PDHc-E1 with PDHc-E2, (D) Δ16−25 PDHc-E1 in the presence of PDHc-E2, and (E) Arg14Ala PDHc-E1 in the presence of PDHc-E2.

Addition of PDHc-E2 to the Δ46−55 variant of PDHc-E1 gave results similar to that observed with parental PDHc-E1. In contrast, incubation of Δ16−25, Δ26−35, and Δ36−45 variants of PDHc-E1 with PDHc-E2 did not produce the same high-molecular weight species with a retention time of 11.8 min. Peaks with retention times of 15.9 min (Δ16−25), 15.2 min (Δ26−35), and 15.6 min (Δ36−45) corresponding to PDHc-E1 dimers were observed, indicating that deletions in the N-terminal region corresponding to amino acids 16−45 have an important impact on the interaction of PDHc-E1 with PDHc-E2. The elution profile for Δ16−25 PDHc-E1 in the presence of PDHc-E2 is presented in Figure 3D. It is notable that the peak at 25 min corresponding to a partially folded Δ16−25 PDHc-E1 (see the previous paragraph) is strongly enhanced at the expense of the Δ16−25 PDHc-E1 dimer peak on addition of PDHc-E2 (compare panels B and D of Figure 3; all deletion variants displayed the same behavior).

Size-exclusion HPLC studies on the complexation of PDHc-E1 and PDHc-E2 were also carried out with the singly substituted PDHc-E1 variants. The Pro10Ala, Ile11Ala, and Thr13Ala variants were apparently converted quantitatively to the complex on addition of PDHc-E2, as is parental PDHc-

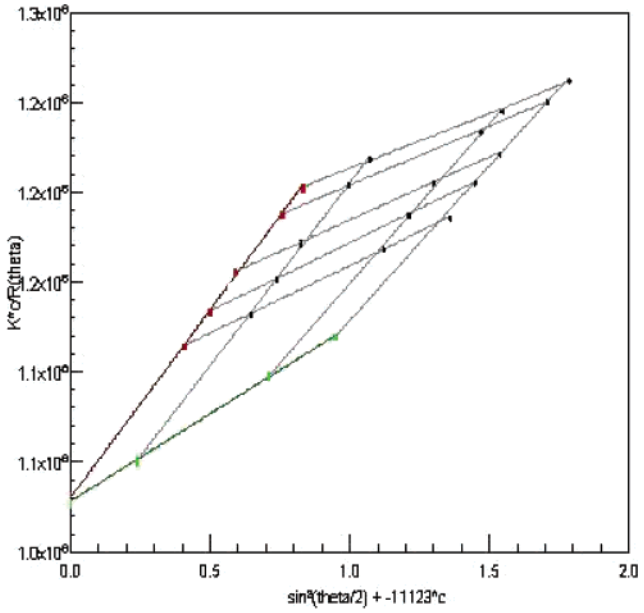

FIGURE 4: Dynamic light scattering experiments (Zimm plot) for determination of the M_r of the complex formed between PDHc-E1 and PDHc-E2. Molecular weight determinations were acquired on the peak from the size-exclusion HPLC column with a retention time of 11.8 min (Figure 3C) at protein concentrations of 1.98, 5.94, and 7.92 μg/mL dissolved in 50 mM KH_2PO_4 containing 0.15 M NaCl (pH 7.0) and scattering angles of 79.7°, 90°, 100.3°, 121.2°, and 132.2°. The M_r and the rms radius were 972 300 ± 4100 and 32.2 ± 0.4 nm, respectively.

E1. With the Asp7Ala, Asp9Ala, Glu12Gln, Glu12Asp, Arg14Ala, and Asp15Ala variants, the mostly uncomplexed PDHc-E1 dimer was in evidence (see Figure 3E for the Arg14Ala variant in complex with PDHc-E2 as an example of the observed data). According to SDS−PAGE, the peak at 11.6 min observed in Figure 3E pertains to PDHc-E2. Similar data were obtained for the Asp7Ala, Asp9Ala, Glu12Gln, Glu12Asp, and Asp15Ala variants, indicating that these substitutions weakened the interaction between PDHc-E1 and PDHc-E2.

The PDHc-E1−PDHc-E2 subcomplex identified in the size-exclusion HPLC chromatogram for parental PDHc-E1 (elution time of 11.8 min, Figure 3C) was also subjected to multiangle laser light scattering experiments, yielding an M_r of 972 300 ± 4100 according to the Zimm plot (Figure 4). Since the mass of PDHc-E1 equals 99 474 Da and that of PDHc-E2 equals 45 802 Da, this value is consistent with either a 3:6 $(PDHc\text{-}E1)_2$:PDHc-E2 ratio or a 4:4 $(PDHc\text{-}E1)_2$:PDHc-E2 ratio. An estimate from the Debye equation at different protein concentrations gave an average of 919 000 ± 12 700. For comparison, similar studies were carried out on PDHc-E1, giving an M_r of 169 000 ± 15 900.

Test for the Ability of PDHc-E1 Deletion Constructs To Reductively Acetylate the Independently Expressed Lipoyl Domain and PDHc-E2 Subunit. Recently, we reported a method for monitoring the reductive acetylation of the independently expressed lipoyl domain and of PDHc-E2 by PDHc-E1 and pyruvate by using MALDI-TOF mass spectrometry (*11*, *17*). The molecular mass of the independently expressed lipoyl domain determined by MALDI-TOF was 8982 ± 4 Da, in good agreement with the theoretical mass of 8975 Da (*17*). Within 30 s of incubation of the lipoyl domain with parental PDHc-E1 and pyruvate, the acetylated form of the lipoyl domain with a molecular mass of 9019 ± 2 Da was observed (*11*, *17*). However, with H407A PDHc-E1, the time course of interconversion of unacetylated and acetylated forms of the lipoyl domain could be monitored by MALDI-TOF (*11*), leading to a pseudo-first-order rate constant for reductive acetylation of the lipoyl domain of 0.0038 s^{-1} and indicating that this method could be used for quantification of this reaction rate.

Table 3: Acetylation of the Lipoyl Domain by PDHc-E1 and Its Deletion and Singly Substituted Variants According to MALDI-TOF MS

enzyme variant	mass of the lipoyl domain (Da)[a] at 1 min	mass of the lipoyl domain (Da)[a] at 30 min	mass of the lipoyl domain (Da)[b] from PDHc-E_2 at 30 min
PDHc-E1	9019.00	9019.00	10159.00
Δ16−25	9026.71	9024.35	10169.92
Δ 26−35	9033.62	9034.48	10161.85
Δ 36−45	9024.46	9022.38	10157.92
Δ 46−55	*c*	9031.40	10180.91
Asp7Ala	9022.72	9019.81	*c*
Asp 9Ala	9021.73	9013.06	101.58
Pro10Ala	9019.94	9019.01	10145.79
Ile11Ala	9021.15	9017.50	*c*
Glu12Gln	9028.35	9021.88	*c*
Glu12Asp	9014.03	9022.06	*c*
Thr13Ala	9027.31	9022.72	10149.96
Arg14Ala	9030.53	9026.11	10151.30
Asp15Ala	9028.83	9021.59	*c*

[a] Independently expressed lipoyl domain. [b] Lipoyl domain resulting from the tryptic digest of PDHc-E2 with a single lipoyl domain (*17*). [c] Not available.

We used the same method to show that the Δ16−25, Δ26−35, Δ36−45, and Δ46−55 variants of PDHc-E1 could all acetylate the lipoyl domain after incubation for 30 min, and that even within 1 min of incubation only the acetylated forms of the lipoyl domain could be detected (Table 3). The results suggest that these deletions do not significantly affect the reductive acetylation. Similarly, the mass of the lipoyl domain derived from PDHc-E2 (molecular mass of 10 112 ± 3 Da), after tryptic digestion of a PDHc-E1−PDHc-E2 complex that had been first incubated with pyruvate for 30 min at 25 °C, indicated full acetylation (the molecular mass of the acetylated lipoyl domain released by tryptic digestion was 10 159 ± 3 Da). Apparently, all PDHc-E1 deletion variants could still reductively acetylate both the independently expressed lipoyl domain and PDHc-E2.

All singly substituted variants of PDHc-E1 could reductively acetylate the independently expressed lipoyl domain after incubation for 1 min (Table 3). It was shown that after incubation of Asp9Ala, Pro10Ala, and Thr13Ala variants of PDHc-E1 for 1 min with PDHc-E2, the lipoyl domain derived from PDHc-E2 was in its acetylated form (not presented), notwithstanding the fact that some of these variants had very low overall activity (Table 2). With the Arg14Ala variant, full acetylation was noted after incubation with PDHc-E2 for 30 min (mass = 10151 Da) (Table 3).

As a control for the experiments presented above, we asked whether PDHc-E1 from *Mycobacterium tuberculosis* (PDHc-E1mt; 52% identical with *E. coli* PDHc-E1) could also reductively acetylate the lipoyl domain and E2 from *E. coli* (PDHc-E1mt was expressed and purified in our laboratory; to be presented elsewhere). Remarkably, *PDHc-E1mt did acetylate the E. coli lipoyl domain expressed independently*

(*mass of the lipoyl domain was 9023.68), but did not acetylate the E. coli PDHc-E2* even after incubation for 40 min (mass of the detected lipoyl domain was 10 103), indicating that specific recognition of the E2 subunit by its cognate PDHc-E1 is important for its reductive acetylation.

Thermochemical Stability of PDHc-E1 and Its Deletion Variants. The T_m of each truncated variant of PDHc-E1 was determined using DSC. The T_m values deduced from these studies were as follows: 50.81 °C for parental PDHc-E1, 50.47 °C for Δ16−25, 49.94 °C for Δ26−35, 50.25 °C for Δ36−45, and 50.91 °C for Δ46−55. Apparently, the stability of each deletion variant was very similar to that of parental PDHc-E1.

DISCUSSION

In this paper, we present evidence for the N-terminal region of the PDHc-E1 subunit from *E. coli* playing a major role in the interaction with the PDHc-E2 subunit. On the basis of the FT-ICR MS results, we concluded that PDHc-E2 protects N-terminal residues 1−55 of PDHc-E1 selectively from trypsin digestion, notwithstanding the fact that the sequence spanning residues 1−55 gives no interpretable electron density in the high-resolution X-ray structure of *E. coli* PDHc-E1 (*10*). This information, along with results on the related enzyme from *Azotobacter vinelandii* (*12*−*14*), prompted us to undertake studies of deletion constructs and single-amino acid substitutions in this amino-terminal region of PDHc-E1.

The following could be concluded regarding the behavior of PDHc-E1 with deletions and single-amino acid substitutions in amino-terminal residues 1−55.

(1) N-Terminal residues 1−15 of PDHc-E1 from *E. coli* appear to have several hot spots that are important for structure and function, as seen with the singly substituted variants in this paper, and the fact that Δ6−15 PDHc-E1 and an N-terminally histidine-tagged construct could not be expressed.

(2) PDHc-E1 functions as a dimer in aqueous solution and appears as a symmetrical dimer in the X-ray crystal structure (*10*). The size-exclusion chromatographic studies clearly showed that the amino-terminal PDHc-E1 deletions and substitutions did not abolish the ability to dimerize.

(3) The ability to decarboxylate pyruvate in the E1-specific DCPIP assay is only modestly affected, indicating that these can still bind ThDP and can also decarboxylate pyruvic acid. We conclude that these amino-terminal residues have only a minor role in the reaction through decarboxylation (eq 1).

(4) The overall PDHc activity monitored by NADH production after reconstitution of the entire complex (reactions after the decarboxylation step) is very much affected by both the deletions and the single-amino acid substitutions at Asp7, Asp9, Glu12, Thr13, Arg14, and Glu15. This entire region must be required in the reaction sequence between the reductive acetylation of lipoamide E2 and the recycling to oxidized lipoamide E2 via PDHc-E3.

Since the PDHc-E2 subunit forms the core of PDHc with PDHc-E1 and PDHc-E3 assembling around it (*1*, *2*, *13*), and there is no direct communication between PDHc-E1 and PDHc-E3, it is very likely that the N-terminus of *E. coli* PDHc-E1 is involved in binding to PDHc-E2 in a manner similar to that suggested for *A. vinelandii* E1 (*14*).

Surprisingly, according to MALDI-TOF MS, the deletions between residues 16−55 and single-amino acid substitutions in N-terminal residues 7−15 of PDHc-E1 did not impair the ability to reductively acetylate either the independently expressed lipoyl domain or the 1-lipoyl E2 construct, which we have shown to be nearly as active in all respects *in vitro* as the 3-lipoyl E2 present in *E. coli* PDHc. This suggests that the reductive acetylation of PDHc-E2 by the amino-terminal PDHc-E1 variants was not seriously affected on the time scale used for the overall assay of the entire complex. The suggestion from these very useful experiments is that a step beyond reductive acetylation is impacted by the interaction monitored below (i.e., a reaction after eq 2).

Size-exclusion HPLC experiments very powerfully indicated that a PDHc-E1−PDHc-E2 complex was being formed between PDHc-E2 and parental PDHc-E1 or its Δ46−55, Pro10Ala, Ile11Ala, etc. However, this complex was no longer being formed in detectable amounts between PDHc-E2 and the Δ16−25, Δ26−35, and Δ36−45 deletion variants, and with the Asp7Ala, Asp9Ala, Glu12Asp, Arg14Ala, and Asp15Ala substitutions.

In conjunction with the studies on the reductive acetylation in the previous paragraph, the most plausible explanation of these results, as well as of the overall PDHc activity results, is that with the deletions carried out, the interaction between PDHc-E1 and PDHc-E2 is virtually abolished. Significantly, the results identify residues 7−45 as being important for this interaction.

The results from dynamic light scattering experiments suggest that parental PDHc-E1 and PDHc-E2 can form a complex very much smaller than that suggested for *E. coli* PDHc [24E1−24E2−12E3 (*1*)], while the size-exclusion chromatographic results suggest that in the presence of PDHc-E1, PDHc-E2 may become more structured, or at least the complex between the two is structured. The 3:6 $(PDHc\text{-}E1)_2$:PDHc-E2 stoichiometry is consistent with structural studies of the E2 core from the related *A. vinelandii*, which suggests that the E2 core forms trimers and multiples of trimers (*13*).

The results with singly substituted variants revealed further evidence of a new feature we had not observed before, stabilization of PDHc-E2 by addition of the PDHc-E1 variant without formation of a stable complex between them. This was established by examination of SDS−PAGE for chromatograms as shown in Figure 3, which indicated the peak at 11.8 min in Figure 3C consisted of essentially equal intensity bands for PDHc-E1 and PDHc-E2, while the peak at 11.6 min in Figure 3E consisted of PDHc-E2. This shows that the structure of PDHc-E2 is influenced by PDHc-E1 even when there is no stable complex being formed between the two. These results, when compared with those obtained with the deletion variants, also demonstrate that an intact N-terminal region of PDHc-E1 is required for stabilizing PDHc-E2.

The relationship of our work to studies on the N-terminal region of PDHc-E1 from *A. vinelandii* is relevant in view of the observed degree of sequence identity (Figure 2). In a series of papers, de Kok and co-workers carried out studies to identify the interaction locus between PDHc-E1 and PDHc-E2 of *A. vinelandii* (*12*−*14*). Three nonconserved amino acids were substituted in an attempt to define which are important for the interaction and which determine

specificity (*14*). Of the three substitutions (specific activity in parentheses), Asp17Arg (1%) and Asp24Arg (10%) were found to be more important than Asp20Gln (83%). In contrast, we mapped the entire region of residues 7−55 of *E. coli* PDHc-E1 with single-amino acid substitutions of seven residues, of which Asp7, Asp9, Pro10, Glu12, Thr13, and Asp15 (the latter is Asp or Glu in all of the sequences) are highly conserved in Gram-negative bacteria. These conserved residues on PDHc-E1 from *E. coli* are now shown to be among those responsible for binding the protein to PDHc-E2, though they do not impart selectivity. Conclusions similar to those reached here for *E. coli* PDHc-E1 were reached with PDHc-E1 from *A. vinelandii* on the basis of a construct in which the 48 N-terminal amino acids were deleted (*12*); hence, these findings appear to be generally significant to PDH complexes with α_2 E1 structures. However, as discussed above, the behavior of the deletion and singly substituted variants led to distinct information with regard to both E1 and E2 subunits.

So far, no structural information about where on *E. coli* PDHc-E2 the PDHc-E1 interacts is available. On the related enzyme from *A. vinelandii* (also forms an octahedral complex with an α_2 E1 structure), it was suggested that E1 interacts with two regions of the E2 subunit, the peripheral subunit-binding domain and the catalytic domain (*18*). In contrast, E1 from *Bacillus stearothermophilus* (forms an icosahedral complex with E1 having an $\alpha_2\beta_2$ structure) (*19*) was suggested to bind only to the peripheral subunit-binding domain of E2.

We conclude that there are at least two loci of interaction between the PDHc-E1 and PDHc-E2 subunits in *E. coli*: (1) an interaction between the thiamin diphosphate-bound substrate on PDHc-E1 and the lipoylamide of PDHc-E2, as reflected by the ability to reductively acetylate the latter, and (2) an interaction of amino-terminal residues 1−45 of PDHc-E1 with regions of PDHc-E2 (so far undefined for the *E. coli* complex), as reflected by the overall activity of the entire complex. Apparently, the first interaction is necessary but not sufficient for completion of the series of reactions carried out by the pyruvate dehydrogenase complex, and can occur even in the absence of the second interaction, which is required for multiple turnovers. We also conclude that the second locus on PDHc-E2 is more important for dictating the specificity of interaction with PDHc-E1, according to our observation that PDHc-E1mt and pyruvate could reductively acetylate the lipoyl domain, but not PDHc-E2 from *E. coli*. Similar conclusions were reached in a paper comparing the interaction of *E. coli* subunits with those of the *A. vinelandii* complex (*14*).

ACKNOWLEDGMENT

We are grateful to Dr. Frieder Jaekle for help with the light scattering experiments and Dr. Alexander Volkov for advice with the mutagenesis studies. We also acknowledge a collaboration with Drs. John Blanchard and Argyrides Argyrou on the complex from *M. tuberculosis*.

REFERENCES

1. Reed, L. J. (1974) Multienzyme Complexes, *Acc. Chem. Res. 7*, 40−46.
2. Perham, R. N. (2000) Swinging arms and swinging domains in multifunctional enzymes: catalytic machines for multistep reactions, *Annu. Rev. Biochem. 69*, 961−1004.
3. Jordan, F. (2003) Current Mechanistic Understanding of Thiamin Diphosphate-dependent Enzymatic Reactions, *Nat. Prod. Rep. 20*, 184−201.
4. Furey, W., Arjunan, P., Brunskill, A., Chandrasekhar, K., Nemeria, N., Wei, W., Yan, Y., Zhang, S., and Jordan, F. (2004) Structure and Intersubunit Information Transfer in the *Escherichia coli* Pyruvate Dehydrogenase Multienzyme Complex, in *Thiamine: Catalytic Mechanisms and Role in Normal and Disease States* (Jordan, F., and Patel, M., Eds.) pp 407−432, Marcel Dekker, New York.
5. Stephens, P. E., Darlison, M. G., Lewis, H. M., and Guest, J. R. (1983) The Pyruvate Dehydrogenase Complex of *Escherichia coli* K12. Nucleotide Sequence Encoding the Pyruvate Dehydrogenase Component, *Eur. J. Biochem. 133*, 155−162.
6. Stephens, P. E., Darlison, M. G., Lewis, H. M., and Guest, J. R. (1983) The Pyruvate Dehydrogenase Complex of *Escherichia coli* K12. Nucleotide Sequence Encoding the Dihydrolipoamide Acetyltransferase Component, *Eur. J. Biochem. 133*, 481−489.
7. Russell, G. C., Machado, R. S., and Guest, J. R. (1992) Overproduction of the Pyruvate Dehydrogenase Multienzyme Complex of *Escherichia coli* and Site-Directed Substitutions in the E1p and E2p Subunits, *Biochem. J. 287*, 611−619.
8. Yi, J., Nemeria, N., McNally, A., Jordan, F., Guest, J. R., and Machado, R. (1996) Effect of Mutations in the Thiamin Diphosphate-Mg Fold on the Activation and Inhibition of the Pyruvate Dehydrogenase Complex from *E. coli*, *J. Biol. Chem. 271*, 33192−33200.
9. Stephens, P. E., Lewis, H. M., Darlison, M. G., and Guest, J. R. (1983) Nucleotide Sequence of the Lipoamide Dehydrogenase gene of *Escherichia coli* K12, *Eur. J. Biochem. 135*, 519−527.
10. Arjunan, P., Nemeria, N., Brunskill, A., Chandrasekhar, K., Sax, M., Yan, Y., Jordan, F., Guest, J. R., and Furey, W. (2002) Structure of the Pyruvate Dehydrogenase Multienzyme Complex E1 Component from *E. coli* at 1.85 Å Resolution, *Biochemistry 41*, 5213−5221.
11. Nemeria, N., Arjunan, P., Brunskill, A., Sheibani, F., Wei, W., Yan, Y., Zhang, S., Jordan, F., and Furey, W. (2002) Histidine 407, a Phantom Residue in the E1 Subunit of the *Escherichia coli* Pyruvate Dehydrogenase Complex, Activates Reductive Acetylation of Lipoamide on the E2 Subunit. An Explanation for Conservation of Active Sites between the E1 Subunit and Transketolase, *Biochemistry 41*, 15459−15467.
12. Hengeveld, A. F., Schoustra, S. E., Westphal, A. H., and de Kok, A. (1999) Pyruvate Dehydrogenase from *Azotobacter vinelandii*: Properties of the N-terminally truncated enzyme, *Eur. J. Biochem. 265*, 1098−1107.
13. de Kok, A., Hengeveld, A. F., Martin, A., and Westphal, A. H. (1998) The pyruvate dehydrogenase multi-enzyme complex from Gram-negative bacteria, *Biochim. Biophys. Acta 1385*, 353−366.
14. Hengeveld, A. F., and de Kok, A. (2002) Identification of the E2-binding residues in the N-terminal domain of E1 of a prokaryotic pyruvate dehydrogenase complex, *FEBS Lett. 522*, 173−176.
15. Nemeria, N., Yan, Y., Zhang, Z., Brown, A., Furey, W., Guest, J., and Jordan, F. (2001) Inhibition of the *E. coli* Pyruvate Dehydrogenase Complex-E1 Subunit and its Tyrosine 177 Variants by Thiamin 2-Thiazolone and Thiamin 2-Thiothiazolone Diphosphates: Evidence for Reversible Tight-Binding Inhibition, rather than Transition-state analogue Behavior, *J. Biol. Chem. 276*, 45969−45978.
16. Nemeria, N., Volkov, A., Brown, A., Yi, J., Zipper, L., Guest, J. R., and Jordan, F. (1998) Systematic Study of all Six Cysteines of the E1 Subunit of the Pyruvate Dehydrogenase Multienzyme Complex from *Escherichia coli*: None is Essential for Activity, *Biochemistry 37*, 911−922.
17. Wei, W., Li, H., Nemeria, N., and Jordan, F. (2003) Expression and Purification of the Dihydrolipoamide Acetyltransferase and Dihydrolipoamide Dehydrogenase Subunits of the *Escherichia coli* Pyruvate Dehydrogenase Multienzyme Complex. A Mass Spectrometric Assay for Reductive Acetylation of Dihydrolipoamide Acetyltransferase, *Protein Expression Purif. 28*, 140−150.
18. Schulze, A., Westphal, A. H., Boumans, H., and deKok, A. (1991) Site-directed mutagenesis of the dihydrolipoyl transacetylase

component (E2p) of the pyruvate dehydrogenase complex from *Azotobacter vinelandii*. Binding of the peripheral components E1p and E3, *Eur. J. Biochem. 202*, 841−848.
19. Mande, S. S., Sarfaty, S., Allen, M. D., Perham, R. N., and Hol, W. G. J (1996) Protein−protein interactions in the pyruvate dehydrogenase multienzyme complex: dihydrolipoamide dehydrogenase complexed with the binding domain of dihydrolipoamide acetyltransferase, *Structure 4*, 277−286.

BI049027B